



LAWRENCE
LIVERMORE
NATIONAL
LABORATORY

High pressure nano-crystalline microstructure of shock compressed single crystal iron

J. Hawreliak, D. Kalantar, J. Stolken, B.
Remington, H. Lorenzana, J. Wark

December 13, 2007

Physical Review B

Disclaimer

This document was prepared as an account of work sponsored by an agency of the United States government. Neither the United States government nor Lawrence Livermore National Security, LLC, nor any of their employees makes any warranty, expressed or implied, or assumes any legal liability or responsibility for the accuracy, completeness, or usefulness of any information, apparatus, product, or process disclosed, or represents that its use would not infringe privately owned rights. Reference herein to any specific commercial product, process, or service by trade name, trademark, manufacturer, or otherwise does not necessarily constitute or imply its endorsement, recommendation, or favoring by the United States government or Lawrence Livermore National Security, LLC. The views and opinions of authors expressed herein do not necessarily state or reflect those of the United States government or Lawrence Livermore National Security, LLC, and shall not be used for advertising or product endorsement purposes.

High pressure nano-crystalline microstructure of shock compressed single crystal iron

James A. Hawreliak,^{*} Daniel H. Kalantar, James S. Stölken, Bruce A. Remington, and Hector E. Lorenzana
Lawrence Livermore National Laboratory, Livermore, CA , 94550, USA

Justin S. Wark

Department of Physics, Clarendon Laboratory, University of Oxford, Parks Road, Oxford, OX1 3PU, UK

(Dated: December 30, 2008)

We discuss the first grain size measurements made during shock compression using in situ x-ray diffraction. Our experiments have shown unambiguously that single crystal iron shock loaded above 13 GPa along the [100] direction will transform from the ambient α -phase (BCC) to a highly ordered polycrystalline ϵ -phase (HCP). Here, we present a detailed shape analysis of the diffraction peaks using a modified Warren-Averbach method to quantify the microstructure of shock compressed high pressure iron. The ϵ -phase was determined through this method to have grain sizes between of 2 and 15 nm, in reasonable agreement with results from large scale MD simulations. We conclude that single crystal iron becomes nano-crystalline in shock transforming from the α to ϵ phase.

PACS numbers: Valid PACS appear here

The impact of the atomic arrangement on materials properties subjected to high levels of stress and temperature has been studied for nearly a century[1]. Structural changes have been shown to occur in quasi-static experiments, like compression in a diamond anvil cell [2], as well as highly dynamic situations, like shock loading [3]. While atomic arrangement is of crucial importance, it is one of several key attributes that play central roles in determining complicated material properties, such as strength and failure [4]. With respect to these latter two properties, the microstructure of a material can significantly affect material performance, specially at high pressures and high strain rate conditions. A recognized phenomena known to dramatically increase material strength with decreasing grain size is the Hall-Petch effect [5, 6]. It follows that our ability to fundamentally understand and predict material behavior in extreme environments depends partially but crucially on understanding the microstructure of the high pressure state of a solid. While literature exists describing residual defect microstructure of samples upon recovery from shock experiments [7, 8], the insight such post-shock measurements afford is fundamentally limited by the dynamic release process after the pressure pulse, which can radically reduce defect densities and alter the microstructure from that which was present under peak transient compression. To date, there have been no reported in situ measurements of the microstructure during shock loading due to the experimental challenges associated with in situ measurements of microstructure. Accordingly, a measurement of grain size would constitute a critical step in developing a basic understanding of microstructure dependence on loading history and equation of state. In this paper we describe an in situ measurements of microstructure for a dynamically loaded material by use of

x-ray diffraction from the high pressure phase of shock compressed single crystal iron. We describe a unique nano-crystalline material which is highly textured that exists only in a high pressure state, generated from single crystal iron under dynamic conditions.

The $\alpha - \epsilon$ phase transition in iron has been one of the most studied high pressure transitions in material science owing to iron's fundamentally and geophysical importance. For the shock physics community it represents a major success as the $\alpha - \epsilon$ phase transition in iron was first detected in shock loading before it was confirmed at a similar pressure under static experiments[9–11]. While the time scale of the applied pressure varies greatly between the dynamic and static experiments, it had always been assumed the transition observed in these experiments were the same. Using in situ x-ray diffraction, we recently confirmed that single crystal iron indeed transforms to the high pressure ϵ -phase [12] when shocked along the [100] direction. A detailed analysis of the ϵ -phase data provided insight into the transition mechanism and the difference in the c/a ratios observed between the transient and static experiments[13]. The transition of iron from bcc to hcp due to shock loading of a single crystal along the [100] direction consists of an elastic compression of the lattice along the [100] direction with the formation of a pseudo-hexagon in the [110] plane. By a shift of alternate (110) planes the hexagons in the (110) BCC planes become (0001) planes in the high pressure HCP system. Due to the symmetry about the compression axis of the BCC lattice it is energetically degenerate for the shuffle of $\{110\}$ planes to occur along any of the four [110] directions, with anti-parallel pairs of [110] shuffles yielding the same orientation of HCP. An example of how this degeneracy in the transition yields a polycrystalline structure is shown in Fig. 1, where the shock direction is into the page. In this figure, we show the α -phase before the transition along with two of the four possible HCP variants. Variant 1, where the shuffle happens in the $[\bar{1}10]$ direction relative to the original

^{*}Electronic address: hawreliak1@llnl.gov

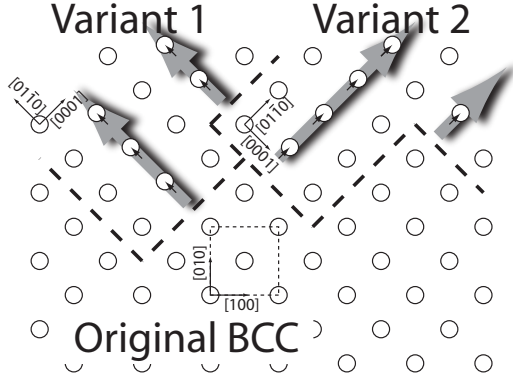


FIG. 1: . A schematic view of the generation of the polycrystalline high pressure ϵ -phase in iron due to the degeneracy of the directions in which the shuffle of alternating planes can occur. In this figure, the shock direction is into the page..

BCC structure establishes the high pressure ϵ -phase with the c -axis along the original $[110]$ direction. Variant 2 occurs due to a shift along the $[110]$ direction and the c -axis along the $[1\bar{1}0]$ direction. While two of the four possible variants are shown it is these variants which lead to a polycrystalline structure of the high pressure phase.

The experiments were performed using the OMEGA[14], Janus, and Vulcan[15] lasers. Samples of 200 - 270 μm thick single crystal $[001]$ iron with a purity of 99.94 % from Accumet Materials and 10 μm thin single crystal foils from the University of Aarhus were coated with a 16–20 μm parylene-N ablator layer followed by a 0.1 μm aluminum shine-through layer. These samples were shock loaded by direct laser irradiation at 2×10^{10} to 1×10^{12} W/cm^2 using 2–6 ns constant intensity laser pulses. The diameter of the region on the crystal shocked by the laser was 2–3 mm. The resulting shock pressure covered a range of pressures that spanned the transition pressure.

The shocked iron single crystals were interrogated by wide-angle in situ diffraction, which has been described extensively elsewhere [16, 17]. In these experiments, a source of 1.85 \AA iron K-shell x-rays was created by laser beams focused on a metal foil synchronous to the shock-driving beams. X-rays were generated from a 100 μm - 200 μm diameter quasi-monochromatic source and diffract from the surface of the crystal 0.7 - 1.3 mm away. The diffracted x-rays were recorded on time integrating film or image plate detector. Figure 2 shows a schematic diagram of the diffraction from a single crystal in this geometry. Temporal resolution in this experiment is provided by varying the duration of the x-ray pulse which closely follows the 2–4 ns optical laser pulse that creates them[18]. For the 200 μm thick iron samples, the X-rays were diffracted only from the shocked-side of the iron crystal in reflection geometry – which we refer to as Bragg geometry. For the 10 μm thin samples it was also possible to record diffracted x-rays in transmission,

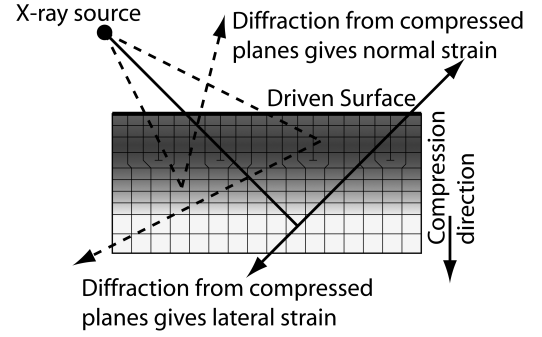


FIG. 2: A schematic diagram of the in situ x-ray diffraction technique. A quasi mono-chromatic source is placed close to a single crystal of material so that x-rays are incident at a wide range of angles. The x-rays diffract from regions of the sample where the Bragg condition is met. A change in angle of the diffracted x-rays indicates a change in the lattice has occurred.

which we refer to as Laue geometry. Owing to the divergence of the x-rays, and the large angle which the crystal subtends to the x-ray source, x-rays diffracted from many different lattice planes in the crystal are simultaneously recorded on two wide angle multiple film packs covering a total of nearly 2π steradians around the sample.[16].

In the raw data shown in Fig 3, the diffracted x-rays appear as curves that are identified with their appropriate plane labels. The 1.85 \AA x-rays have a penetration depth of about 10 μm into the sample. Due to this finite penetration depth and the duration of the x-ray pulse we observe at least two lines associated with each diffraction plane, the unshocked and shock compressed states. The diffraction lines from the unshocked part of the crystal provide a reference from which to measure the change in Bragg angle for each reflection. For shock pressures above the transition pressure, we observe up to two further curves, the first corresponding to elastic compression of the BCC lattice, and the second, broader feature, which is consistent with the period doubling of the BCC structure to HCP. At the highest pressures, however, the crystals are overdriven and the elastic signature is not observed, as in Fig. 3. The diffraction lines from the unshocked lattice are significantly narrower than the shocked diffraction lines, proving that the broadening is not due to the instrument function or the initial state of the crystal. Transmitted x-ray diffraction has shown that the material is polycrystalline in nature by the generation of diffraction lines consistent with different orientations of HCP[12, 13]. We now consider the broadening of the diffraction lines in iron, which can originate from two sources: firstly the finite grain size of the HCP phase, or secondly a strain gradient distribution within the high pressure phase.

The diffuse and continuous nature of the diffraction curves, as seen in Fig 3, sets an upper bound on the possible grain size. In control experiments with the same experimental setup and characterized large grain samples

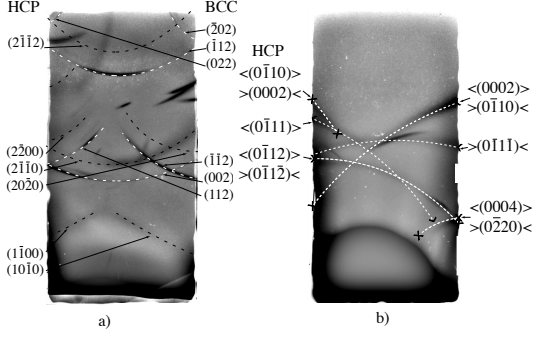


FIG. 3: X-ray diffraction data showing diffraction lines consistent with an HCP high pressure phase in a) Bragg (Reflected) where the static BCC material is denoted with white dashed lines and the higher pressure HCP with black dashed lines and b) Laue (Transmitted) because there is no separation upon compression of the BCC and HCP diffraction planes only the HCP are labelled.

diffraction from individual grains appeared as discrete dashes[19]. Based on this calibration we estimate that we would have observed discrete dashes in our diffraction signal if the grains had been larger than $5 \mu\text{m}$ in the high pressure phase.

To obtain a more refined handle on the grain size we use a modified Warren-Averbach analysis[20] to fit the shape of the diffraction peak of the high pressure iron ϵ -phase. This technique, originally put forward by Warren and Averbach in 1950 [20], uses a Fourier transform of the profile of a collection of diffraction peaks to extract the grain size distribution and strain information used to determine material microstructure. The Fourier transform of the profile of a single diffraction peak is described by the function $A_n(l)$, where n is the transformed variable and l is the length of the scattering vector (i.e. the diffraction plane). This function consist of two components, $A_n(l) = A_n^S A_n^D(l)$. One component, A_n^S , is determined by the size distribution of grains in the sample, which has no dependence on the scattering vector, l , and the second, $A_n^D(l)$, is due to non-uniform strain caused by defects and large scale gross strain gradients which depend on the scattering vector. Each term is dependent on the distribution of grain sizes and strains as described by

$$A_n^S = \frac{1}{N_3} \int_{i=n}^{\infty} (i - n)p(i)di, \quad (1)$$

$$A_n^D(l) = \langle \cos(2\pi l Z_n) \rangle, \quad (2)$$

where $p(i)$ is the probability that a grain has a size i and $p(Z_n)$ is the probability of a strain Z between planes separated by n atomic layers, and the distortion term $A_n^D(l)$ assumes that the strain distribution is symmetric (the anti-symmetric part has been ignored for simplicity). In static experiments it is possible to resolve the peak shapes over 2 orders of magnitude in intensity, yielding high fidelity measurements of many components of the

peak transform [21, 22]. In the dynamic experiments described here, the background x-ray signal due to broad-band emission from the backlighter and emission from the plasma generated by the drive laser limit the signal to noise to a fraction of what is possible in static experiments. To accommodate this we simplify the analysis by assume a single grain size and a Guassian distribution of strain. Then the broadening of the peak is described by [23]

$$A_n^S = \exp\left(-\pi \frac{n^2}{\sigma^2}\right), \quad (3)$$

where σ is the grain size and the strain distribution is described by a single function $p(\epsilon)$ where $\epsilon = Z_n/n$ is the normalized strain and the broadening is

$$A_n^D(l) = \exp(2\pi^2 l^2 n^2 \langle \epsilon^2 \rangle), \quad (4)$$

Using these two approximations, a diffraction peak is described by a Gaussian distribution

$$a(g) = \exp\left(-\frac{g^2}{W^2}\right), \text{ where } W^2 = B^2 + A^2 l^2, \quad (5)$$

and g is the scattering vector associated with the diffraction plane l . By plotting W^2 versus l^2 for a series of peaks, a linear fit results in an estimate of the grain size from the intercept, $B = a_o/\sqrt{\pi}\sigma$ where a_o is the unit cell size, and of the rms strain from the slope, $A = 2\sqrt{2\pi}\sqrt{\langle \epsilon^2 \rangle}$.

In Fig 4, we plot some example data of peak width versus scattering vector. We applied the modified Warren-Averbach analysis to the (1100) and (2200) planes of the high pressure phase which correspond to the original (112) plane and period doubling of the (112) plane (which is forbidden for BCC). We record two orders of the same diffraction plane because the uni-axial nature of the compression could lead to a grain size or strain structure that is highly directionally dependant. Due to the single crystal nature of the sample, diffraction planes with the same directional vectors need to be used to provide a solution for grain size and strain. The plotted widths represent a series of best fitted line outs from the data. While the errors inferred from the experimental data plotted in Fig. 4 appear large, the grain size can still be constrained to an order of 2 to 15 nm, with very low residual strain broadening ($\approx 0.2 \pm 0.8\%$). Also plotted in Fig 4 is a similar analysis applied to simulated x-ray diffraction from large scale MD simulations with a grain size as low as 4 nm for 19.6 GPa shock and as large as 10 nm for the 28.7 and 52.9 GPa shock[24]. The deviation of the MD simulations from a linear fit suggests the strain does not follow a Guassian distribution in the MD simulation. While the determination of a unique strain profile cannot be made in the experiment, the gradual slope of peak width suggests that the dominant mechanism for broadening of the diffraction lines is grain size, both in the experiment and MD simulations.

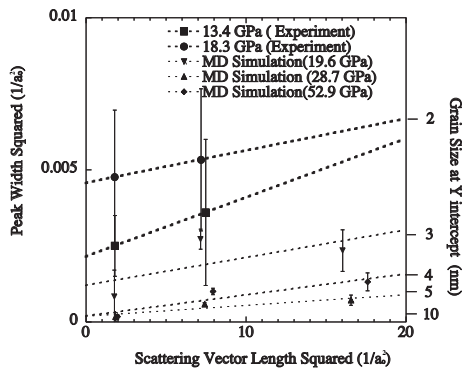


FIG. 4: A plot of the square of the peak widths as a function of the square to the scattering Vector length (the modified Warren Averbach analysis). The gradual slopes of the lines suggests the broadening is dominated by the grain size of the high pressure phase. The right axis label identifies the grain size associated with the peak width, where the y-intercept gives the grain size.

This analysis represents the first measurement of grain size of a material which has undergone a phase transition during dynamic compression using in situ x-ray diffraction. By measuring multiple orders of a diffraction plane simultaneously while the material is under compression, we were able to use a simplified Warren-Averbach analysis to fit the peak broadening of the (1100) and (2200) planes and extract a grain size on the order of 2-15nm with very little residual strain (0.2%). This result is consistent with large scale MD simulations of the $\alpha - \epsilon$ phase transition in iron. Energetically such a highly ordered polycrystalline end state would be expected since four degenerate transition pathways exist for iron compressed along the BCC [100] axis.

Single crystal iron shock compressed along the [100] direction offers a very unique case of a well ordered phase transition. In this case the elastic response of

the atoms before the transition facilitates a compression-shuffle mechanism for the transition, leading to a sub-nanosecond transition to a polycrystalline structure with grains of four orientations. These two orientations with well aligned diffraction planes allows recordable diffraction with a single crystal diagnostic. If the compression were more hydrostatic in nature as suggested by static experiments a different transition mechanism [25] would lead to a more complex final HCP arrangement that may not have been diagnosed with our experimental setup. Large scale MD simulations suggest shock compression along different crystallographic axis (110 and 111) in single crystal iron may lead to a mixed high pressure stage of HCP and FCC with smaller grains [26], which would require polycrystalline diffraction to determine the high pressure structure [27].

Signal to noise levels resulting from these laser based techniques limit the microstructural information that can be extracted on a single shot. With next generation x-ray FEL sources becoming available by 2009, there is the potential to increase the x-ray intensity by a factor of 10^6 (10^3 more photons in 10^3 shorter timescale) [28]. This increase in x-ray signal will yield peak shapes which cover similar intensity scales as those in static experiments, potentially allowing a more detailed analysis of the microstructure using a fuller version of the Warren Averbach technique.

The authors thank the staff at the Vulcan Laser Facility at the Rutherford Appleton Laboratory, the staff at Janus laser at Lawrence Livermore National Laboratory and the staff and University of Rochester Laboratory for Laser Energetics. This work performed under the auspices of the U.S. Department of Energy by Lawrence Livermore National Laboratory under Contract DE-AC52-07NA27344 supported by the LDRD program Project No. 06-SI-004 at LLNL.. Additional support was provided by the DOE under Grants No. DEFG0398DP00212 and No. DEFG0300SF2202, by the U.K. EPSRC under Grant No. GR/R25699/01.

-
- [1] P. W. Bridgman, *Collected experimental papers* (Harvard University Press, Cambridge., 1964).
 - [2] H. Mao, W. A. Bassett, and T. Takahashi, *Journal of Applied Physics* **38**, 272 (1967).
 - [3] J. C. Boettger and D. C. Wallace, *Physical Review B* **55**, 2840 (1997).
 - [4] D. L. Preston, D. L. Tonks, and D. C. Wallace, *Journal of Applied Physics* **93**, 211 (2002).
 - [5] E. O. Hall, *Nature* **173**, 948 (1954).
 - [6] A. H. Chokshi, A. Rosen, J. Karch, and H. Gleiter, *Scr. Metall.* **23**, 1679 (1989).
 - [7] M. A. Meyers, F. Gregori, B. K. Kad, M. S. Schneider, D. H. Kalantar, B. A. Remington, G. Ravichandran, T. Boehly, and J. S. Wark, *Acta Materialia* **51**, 1211 (2003).
 - [8] M. S. Schneider, B. K. Kad, F. Gregori, D. Kalantar, B. A. Remington, and M. A. Meyers, *Metallurgical and Materials Transactions a-Physical Metallurgy and Materials Science* **35A**, 2633 (2004).
 - [9] S. Minshall (1955), vol. 98, p. 271.
 - [10] D. Bancroft, E. L. Peterson, and S. Minshall, *Journal of Applied Physics* **27**, 291 (1956).
 - [11] J. Jamieson and A. W. Lawson, *Journal of Applied Physics* **33**, 776 (1962).
 - [12] D. H. Kalantar, J. F. Belak, G. W. Collins, J. D. Colvin, H. M. Davies, J. H. Eggert, T. C. Germann, J. Hawreliak, B. L. Holian, K. Kadau, et al., *Phys. Rev. Lett.* **95**, 075502 (2005).
 - [13] J. Hawreliak, J. D. Colvin, J. H. Eggert, D. H. Kalantar, H. E. Lorenzana, J. S. Stolken, H. M. Davies, T. C. Germann, B. L. Holian, K. Kadau, et al., *Physical Review B (Condensed Matter and Materials Physics)* **74**, 184107 (2006).
 - [14] T. R. Boehly, R. S. Craxton, T. H. Hinterman, J. H.

- Kelly, T. J. Kessler, S. A. Kumpan, S. A. Letzring, R. L. McCrory, S. F. B. Morse, W. Seka, et al., in *Proceedings of the tenth topical conference on high temperature plasma diagnostics* (AIP, Rochester, New York, 1995), vol. 66, p. 508.
- [15] C. N. Danson, L. J. Barzanti, Z. Chang, A. E. Damerell, C. B. Edwards, S. Hancock, M. H. R. Hutchinson, M. H. Key, S. Luan, and R. R. Mahadeo, *Optics Communications* **103**, 392 (1993).
 - [16] D. Kalantar, E. Bringa, M. Caturla, J. Colvin, K. T. Lorenz, M. Kumar, J. Stolken, A. M. Allen, K. Rosolankova, J. S. Wark, et al., *Review of Scientific Instruments* **74**, 1929 (2003).
 - [17] D. H. Kalantar, E. A. Chandler, J. D. Colvin, R. Lee, B. A. Remington, S. V. Weber, L. G. Wiley, A. Hauer, J. S. Wark, A. Loveridge, et al., *Review of Scientific Instruments* **70**, 629 (1999).
 - [18] D. W. Phillion and C. J. Hailey, *Physical Review A* **34**, 4886 (1986).
 - [19] D. H. Kalantar, J. Belak, E. Bringa, K. Budil, M. Caturla, J. Colvin, M. Kumar, K. T. Lorenz, R. E. Rudd, J. Stolken, et al., *Physics of Plasmas* **10**, 1569 (2003).
 - [20] B. E. Warren and B. L. Averbach, *Journal of Applied Physics* **21**, 595 (1950).
 - [21] T. Ungar and A. Borbely, *Appl. Phys. Lett.* **69**, 3173 (1996).
 - [22] T. Ungar, S. Ott, P. G. Sanders, A. Borbely, and J. R. Weertman, *Acta Materialia* **46**, 3693 (1998).
 - [23] B. E. Warren, *X-ray diffraction* (Dover Publications, New York, 1990), dover ed.
 - [24] K. Kadau, T. C. Germann, P. S. Lomdahl, and B. L. Holian, *Science* **296**, 1681 (2002).
 - [25] F. M. Wang and R. Ingalls, *Physical Review B* **57**, 5647 (1998).
 - [26] K. Kadau, T. C. Germann, P. S. Lomdahl, and B. L. Holian, *Physical Review B* **72**, (2005).
 - [27] J. Hawreliak, H. E. Lorenzana, B. A. Remington, S. Lukezic, and J. S. Wark, *Review of Scientific Instruments* **78**, 083908 (2007).
 - [28] J. Arthur, G. Materlik, R. Tatchyn, and H. Winick, in *Proceedings of the 5th international conference on synchrotron radiation instrumentation* (AIP, Stony Brook, New York (USA), 1995), vol. 66, pp. 1987–1989.